On the construction of a general numerical tyre shear force model from limited data

R. S. Sharp* and M. Bettella**

*Department of Electrical and Electronic Engineering, Imperial College of Science, Technology and Medicine, London SW7 2BT

**Jaguar Cars Engineering Centre, Whitley, Coventry CV3 4LF

Keywords: Tyre, shear force, Magic Formula, normalisation

Abstract: The extension of very limited tyre shear force and moment measured results to allow the modelling and simulation of quite general motions of automobiles is discussed. Relying on a recently devised algorithm, that has its basis in Magic Formula and parameter normalization methods, processes are devised for determining the necessary parameter values of the algorithm. The method is applied to each of two tyres, having substantially different natures. Where data is lacking, fundamental knowledge of tyre mechanics is applied to the problem of obtaining the best values. Results are included to demonstrate the effectiveness of the processes. Data sets for the particular tyres treated and the algorithm itself are included.

NOTATION

b_1-b_{16}; Magic Formula secondary parameters

B_m, B_x, B_y, C, $C_{f\kappa}$, $C_{f\alpha}$, $C_{f\gamma}$, C_m, $C_{m\alpha}$, D_x, D_y, D_{mz}, E, E_m; Magic Formula primary parameters

C_{mz1}, C_{mz2}, C_{mz3}, E_{mz1}, E_{mz2}, E_{mz3}; polynomial coefficients of expressions for C_m and E_m

$\overline{B}, \overline{C}, \overline{E}$; normalised Magic Formula parameters

F_x, F_y, M_z; longitudinal force, lateral force and aligning moment from tyre

F_z; tyre load

g_1; mean ratio of camber stiffness to tyre load

slip_m; normalized slip value for which normalized force is maximum

k, a; longitudinal slip ratio and sideslip angle

κ_p, α_p; slip ratio and slip angle for maximum shear force in pure slip

1 INTRODUCTION

In vehicle dynamics modelling, representing the tyre shear force system properly with respect to the purposes of the activity is well known to be vital. Often, however, tyre shear force data is sparse and it may be prohibitively expensive to obtain directly by measurement. It is therefore of interest to consider the problem of creating a comprehensive shear force model from the kind of limited data that often exists [**1**]. The objective is to use the data, such as it is, to make a general model that will represent real tyre shear force and moment behaviour with generic accuracy. It is also implied that any special tyre force characteristics that may be of interest can be included in the model built, if success is achieved in the main objective.

Several standard vehicle dynamics simulation tests like constant radius turning, the double lane change or the J-turn roll-over test are almost pure lateral tests. In such cases, there is more value in a good representation of the lateral force, compared to the longitudinal one. On the other hand, manoeuvres dominated by braking or driving demand more accuracy from the longitudinal force model, while braking in a turn, for example, requires longitudinal and lateral to be weighted equally.

Recent research [2] has shown that pure slip longitudinal and lateral force data for several tyre loads can be processed in such a way that combined slip forces are derivable from them. A combination of the "Magic Formula" [**3**] and similarity or normalisation methods [**1**, **4**, **5**], together with a new non-linear slip transformation were used. The slip transformation allows both the low slip and high slip shear forces in combined longitudinal and lateral slip to be represented with reasonable accuracy, with a guaranteed smooth transition from braking to cornering. The method involves the adoption of a Magic Formula master curve to represent both longitudinal and lateral forces. When both of these have been measured, it is necessary to compromise between the two, in terms of the accuracy of representation, or to deliberately favour one or the other through the choice of parameter values. The more isotropic a particular tyre is, the less the compromise becomes.

Most commonly, existing data comes in the form of side force against slip angle and aligning moment against slip angle for each of several loads, typically four in number [**1**, **6**]. It is comparatively rare to find corresponding longitudinal force against slip ratio results, partly because some tyre testing rigs are not equipped with braking or driving systems and therefore they are not capable in this respect. Consequently, the present development is aimed at taking side force and aligning moment data for several loads and deriving from them the necessary coefficients to generate a whole spectrum of steady state shear force and aligning moment characteristics. The coefficients are those of the algorithm, devised in reference [**2**] and modified slightly below, which takes load, slip ratio, slip angle and camber angle and gives back longitudinal force, lateral force and aligning moment.

In section 2, the starting data and the processing necessary to derive the coefficients for one particular tyre are explained. A full set of coefficients is derived. In section 3, the coefficients are used to compute combined slip force and moment results and these are shown. In section 4, a second tyre data set is treated in a similar way and corresponding results are given. Conclusions are drawn in section 5.

2 DATA AND PROCESSING FOR A RACE TYRE

The starting point is the data for a Goodyear F1 front tyre, 25.0 x 9.0 – 13 (of some years ago) (given in reference [**1**], figure 2.46). Both side force and aligning moment data were scanned and saved as bitmaps. The maps were then read into MATLAB®, using "imread" and sampled and digitized, using "ginput". The side force data were then used to evaluate C and E, presumed to be the same for each load [**2**], b_4, b_5, relating the cornering stiffness to the load, and b_{13} and b_{14}, relating the peak side force to the load. The relevant equations, from reference [**2**], are:

$$F_y = D_y \sin[C \arctan\{B_y a - E(B_y a - \arctan(B_y a))\}] \quad (1)$$

$$C_{fa} = b_4 \sin(2 \arctan(F_z / b_5)) = B_y C D_y \quad (2)$$

$$D_y = F_z (b_{13}.F_z + b_{14}) \quad (3)$$

The optimization routine "fminsearch" with a sum-of-squares-of-errors objective function was used for this purpose. The original and reconstructed side force / slip angle results are shown in Fig. 1.

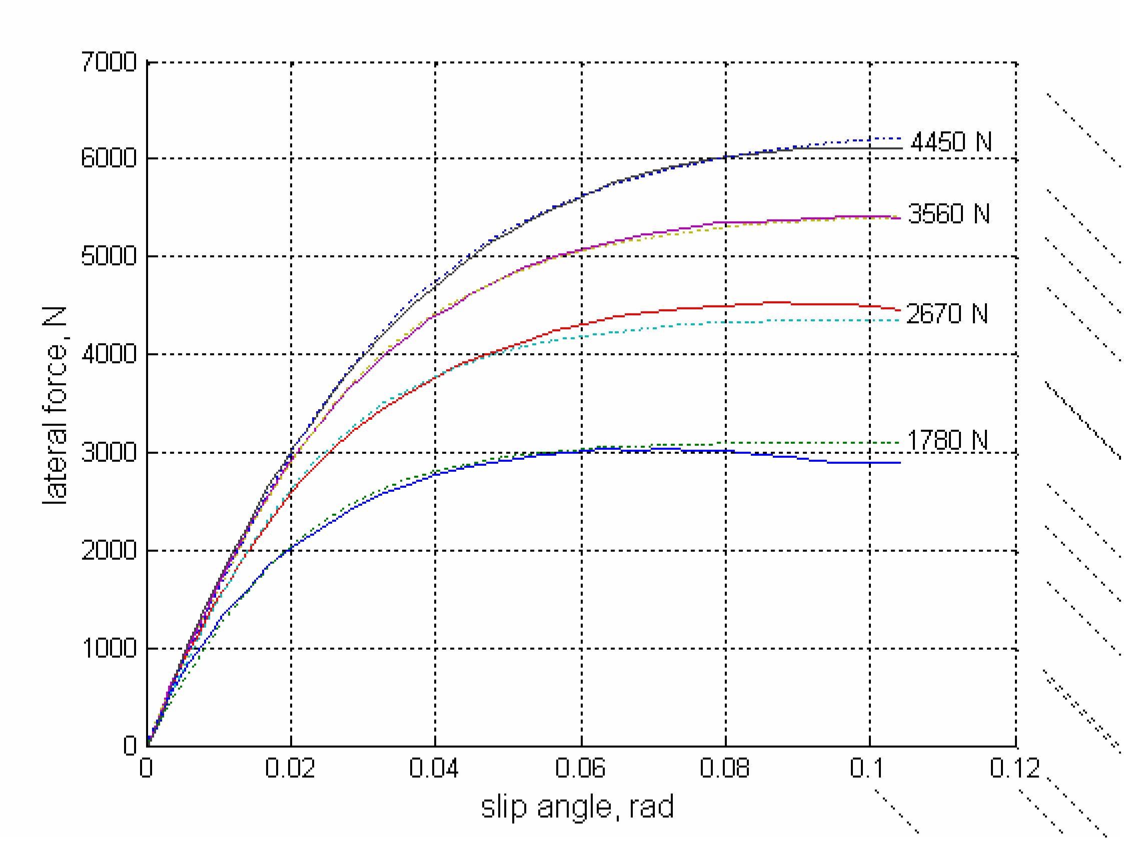

Fig. 1 Original (solid lines) and reconstructed (dotted lines) side force data for Goodyear F1 front tyre, 25.0 x 9.0 – 13 from reference [**1**], with invariant C and E

Parameter values obtained in the error minimization are: C = 1.4125; E = 0.42922; b_4 = 166303; b_5 = 3826.8; b_{13} = -0.00012267; b_{14} = 1.96015. The reconstruction can be seen to be of good quality.

The side force – load data is also used to derive a linear relationship between the slip angle for maximum force and load. The former is obtained by solving the equation [**2**, **3**, **5**]:

$$E = \frac{\{B_y \alpha_p - \tan(\pi/2C)\}}{\{B_y \alpha_p - \arctan(B_y \alpha_p)\}} \qquad (4)$$

for α_p for each load and fitting a straight line to the result. The values and the best fit straight line, are shown in Fig. 2.

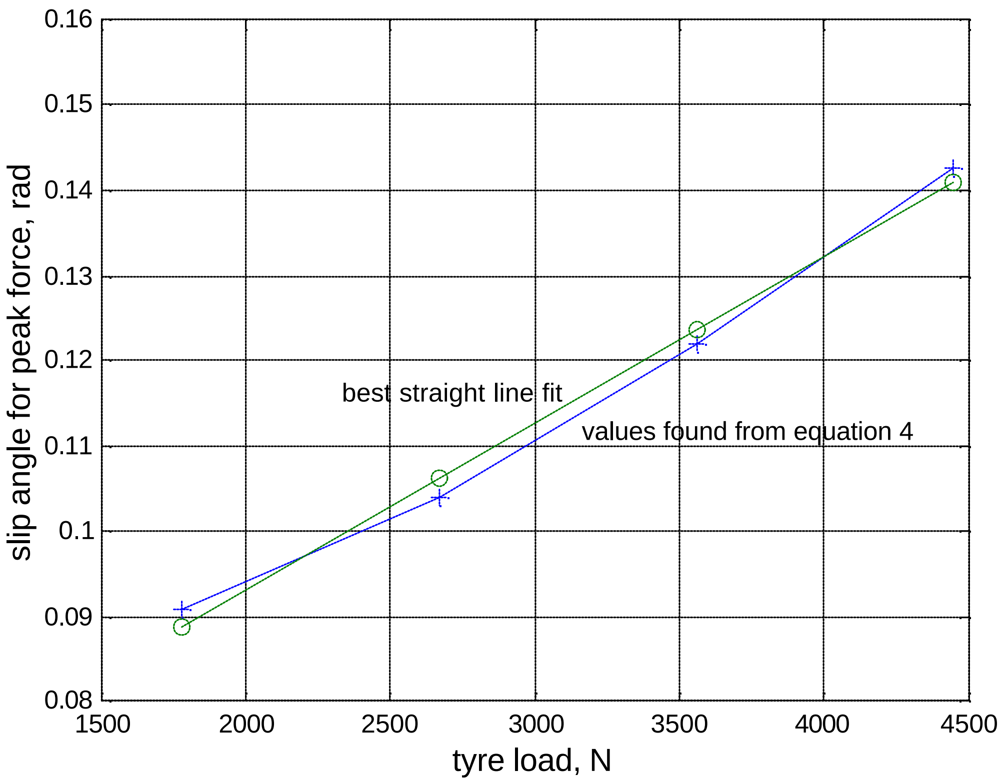

Fig. 2 Values of a_p from solving (4) given B_y, C and E for each of the four standard loads, and its straight line fit: $a_p = 0.000019463.F_z + 0.054238$

The original and reconstructed side force data are shown together in Fig. 3, the slip angle range being much greater than that covered by the measurements. In the typical situation in which the original data spanned only a modest range of slip angles, it can be expected that the value of C from the "best fit" process may not represent the high slip regime especially well. If the parameters were considered unsatisfactory in this respect, C could be fixed and the other parameters could be "optimised" around it.

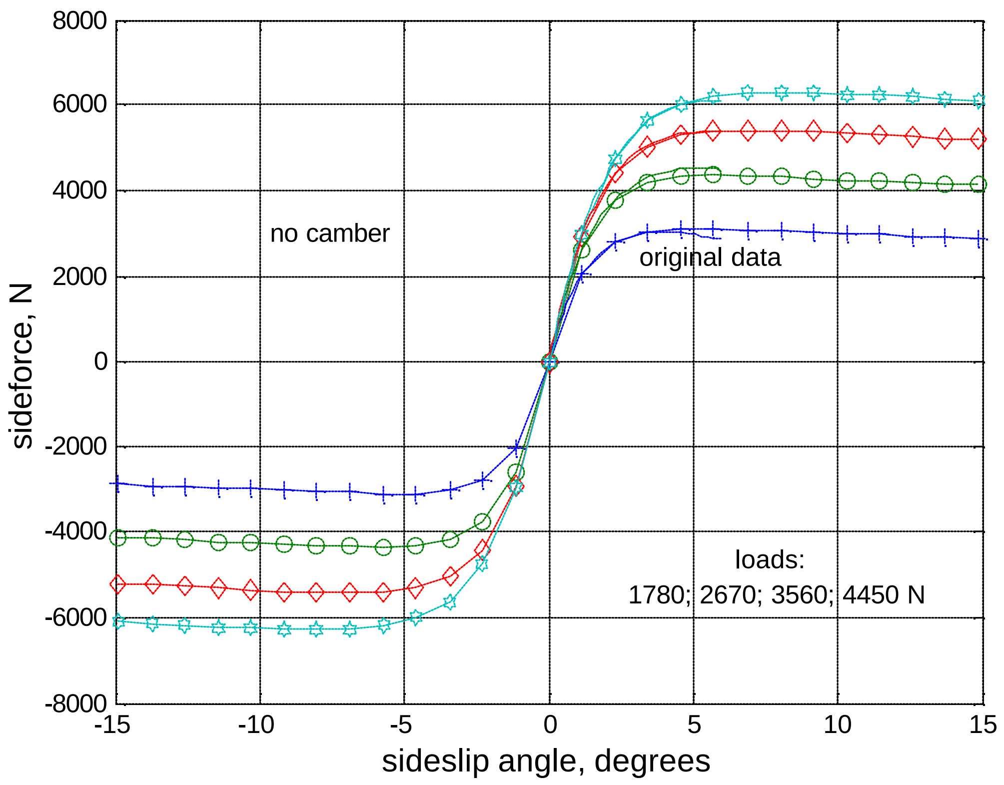

Fig. 3 Side forces as functions of sideslip angle using coefficients from fitting process and showing original data from reference [**1**]

The aligning moment results are next processed in a similar fashion, using the equations:

$$M_z = D_m \sin[C_m \arctan\{B_m a - E_m(B_m a - \arctan(B_m a))\}] \quad (5)$$

$$C_{ma} = F_z(b_6.F_z + b_7)/\exp(b_8.F_z) = B_m C_m D_m \quad (6)$$

$$D_m = F_z\,(b_{15}.F_z + b_{16}) \quad (7)$$

yielding the results of Fig. 4 and the parameter values: C_m = 2.09857; E_m = -0.59291; b_6 = -5.2208e-5; b_7 = 1.9481; b_8 = -4.5687e-5; b_{15} = 8.9894e-6; b_{16} = 3.4000e-3.

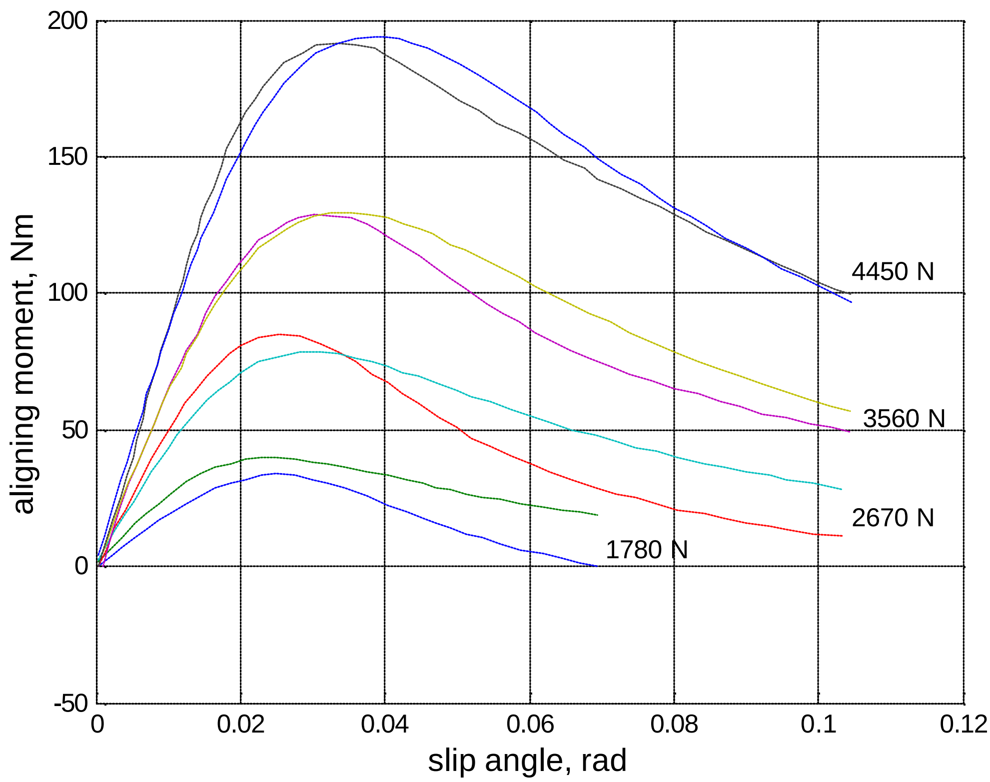

Fig. 4 Original (solid lines) and reconstructed (dotted lines) aligning moment data for Goodyear F1 front tyre, 25.0 x 9.0 – 13 from reference [**1**], with C_m = 2.099 and E_m = -0.5929

The aligning moments for the lower loads are not represented so well and the possibility arises that the fit can be improved by allowing C_m and E_m to vary quadratically with load, as in the full Magic Formula method [**3**, **5**]. This can be done without prejudice to the treatment of the shear forces for combined slip [**2**]. With this more elaborate fitting, the best parameters, for the equations (5) to (7) supplemented by:

$$C_m = C_{mz3} F_z^2 + C_{mz2} F_z + C_{mz1} \tag{8}$$

$$E_m = E_{mz3} F_z^2 + E_{mz2} F_z + E_{mz1} \tag{9}$$

are: C_{mz1} = 2.9000; C_{mz2} = -3.4651e-4; C_{mz3} = 2.4648e-8; E_{mz1} = -1.6529; E_{mz2} = 4.44396e-6; E_{mz3} = -2.3414e-8; b_6 = -4.8699e-5; b_7 = 1.37723; b_8 = -1.2422e-4; b_{15} = 8.0402e-6; b_{16} =

7.7895e-3. The resulting curves are shown in Fig. 5, where the fit can be seen to be much improved.

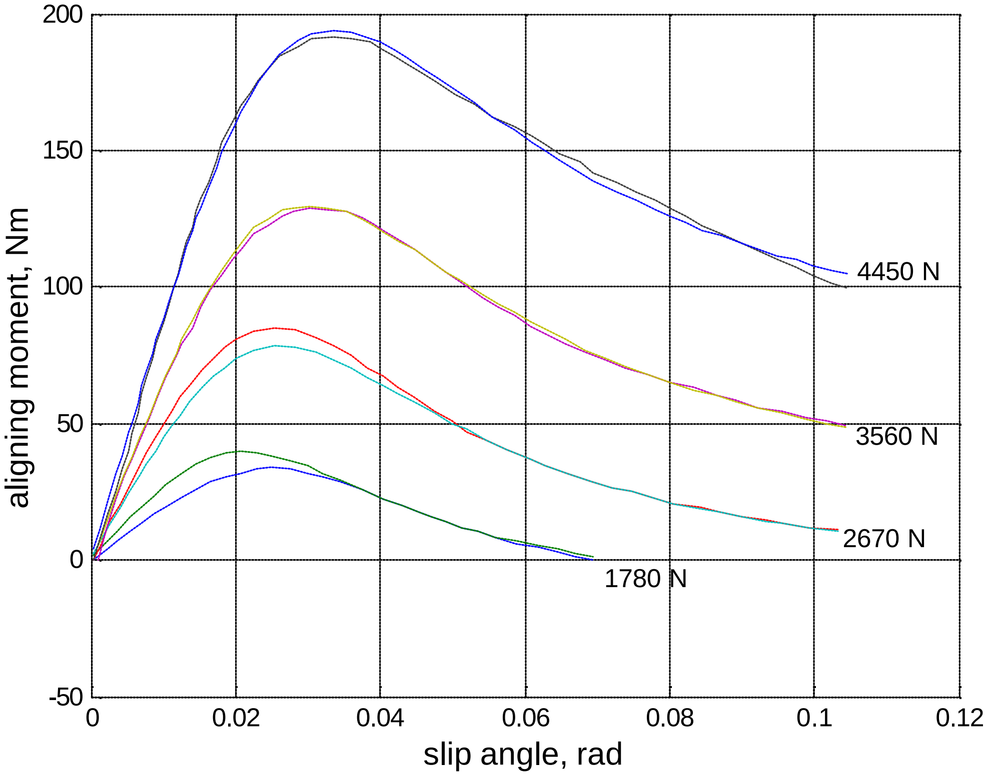

Fig. 5 Original (solid lines) and reconstructed (dotted lines) aligning moment data for Goodyear F1 front tyre, with C_m and E_m made quadratic functions of load

It is now necessary to deal with longitudinal forces. In the absence of any specific measurements of longitudinal forces, it is presumed that the values C and E obtained from the lateral force data belong also to the normalized master curve. This will ensure that the representation of the lateral forces is as accurate as possible. For this master then, $\overline{C} = 1.4125; \overline{E} = 0.42922; \textit{from which}\, \overline{B} = 0.70796$. By solving (4) for this case, slip_m is found to be 3.72715. Next, the peak longitudinal forces are related to the peak lateral forces.

The peaking of the shear forces is associated with the dependence of friction coefficient between rubber and road on the sliding velocity [**7**]. At a certain slip angle or slip ratio, the sliding of the rubber tread elements across the road is such that the shear force is maximized. In the limit when the tyre load is low, the contact between tyre and ground becomes line contact and the optimum sliding condition longitudinally will be the same as that laterally. The peak forces will consequently be the same, which implies that b_{12}, for the longitudinal force, will be equal to b_{14}, for the lateral force with value 1.96015, which value, incidentally, represents the maximum coefficient of friction between the tyre rubber and the ground in the rig test conditions. As the tyre load increases and the contact lengthens, the greater stiffness of the tread base longitudinally will motivate the tread rubber elements towards the same sliding velocity more in longitudinal slip than in lateral slip. The consequence of this is that the longitudinal force peak will be higher and the peak will be sharper [**8**]. It is estimated here that the peak longitudinal force will be 10% higher than the peak lateral force for the highest of the standard loads, 4450 N, which implies that b_{11} = -9.0889e-5.

It is also characteristic of the peak longitudinal forces that they occur at the same slip ratio, typically $\kappa_p = 0.13$, irrespective of load. Presuming the same C and E values (1.4125 and 0.42922 respectively) for lateral force, longitudinal force and master curve and knowing κ_p allows the calculation of B_x from (4). B_x must be constant, since C, E and κ_p are load invariant. This implies that $C_{f\kappa}$, which is $B_x.C.D_x$ varies with load exactly as does D_x, which implies that $b_3 = 0$, $b_1 = B_x.C.b_{11}$ and $b_2 = B_x.C.b_{12}$. Fig. 6 shows the resulting longitudinal forces as functions of slip ratio. Now, we are missing only b_9, b_{10} and g_1 – all to do with wheel camber.

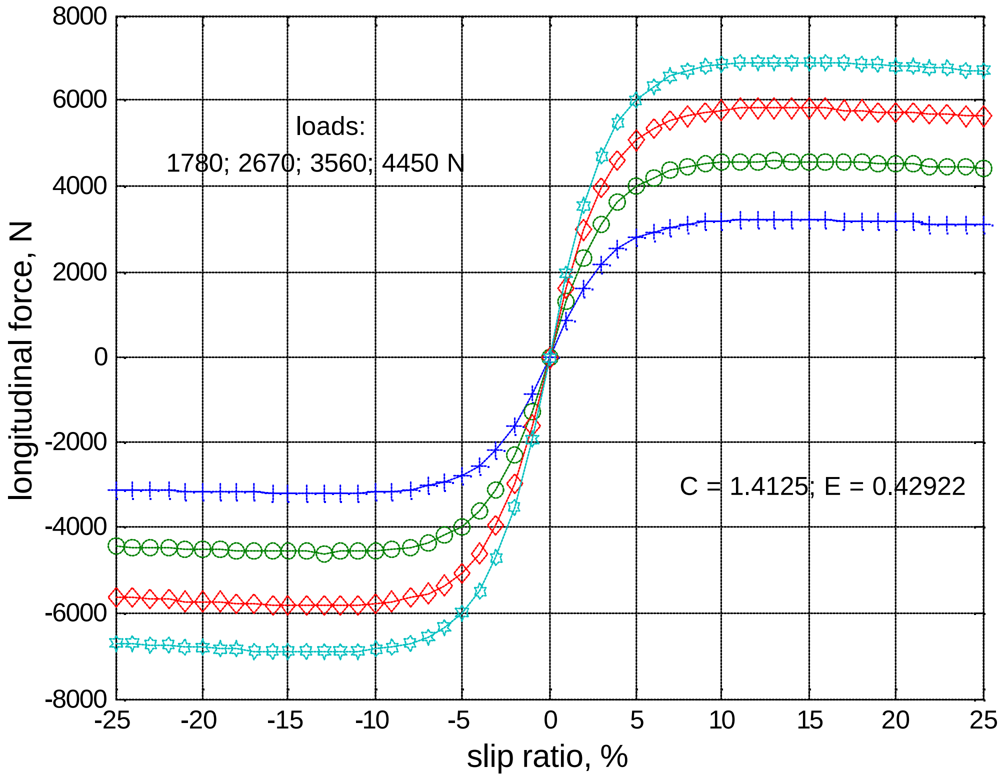

Fig. 6 Longitudinal forces as functions of slip ratio, using selected parameter values

Camber is assumed to influence peak force according to ($g_1.F_z.\gamma$). The topic is treated in reference [**1**] at figures 2.25 and 2.26. 2.25 is for a fixed load, while 2.26 is for each of four loads. The force gain due to camber is very variable over load but taking the mean, g_1 comes to 0.75, not so different from the value of 0.848 given in reference [**8**]. b_9 and b_{10} relate the load to the camber stiffness. Figures 2.28 and 2.29 of reference [**1**] apply. Also, in the limit when the tyre becomes a thin disk, it can be expected that the camber thrust will be equal to the wheel load multiplied by the tangent of the camber angle. (For such a thin disk brush type tyre, from loaded free rolling, with straight contact line and no sideforce, imagine the wheel to be cambered but not so much as to cause sliding in the contact region. Subsequent rolling will maintain the straight contact line. What was previously the load on the tyre will now be a force in the plane of the wheel. That force can be resolved into a vertical load equal to the former load multiplied by the cosine of the camber angle and a camber thrust, which is the former load multiplied by the sine of the camber angle. The ratio of camber thrust to load is now the tangent of the camber angle). In the latter case, b_9 would be zero while b_{10} would be 1, whereas the experimental curves show non-linearity with load, consistent with b_{10} being less than 1 and b_9 being small but positive. To get a reasonable match with the non-linearity in figure 2.28, we take b_9 = 0.00005 and b_{10} = 0.5, compared with 0.00004861 and 0.2537 from reference [**8**].

3 COMBINED SLIP FORCE AND MOMENT RESULTS

These considerations yield a complete data set as follows:

C = 1.4125; B = 1/C; E = 0.42922; slip_m = 3.72715; g_1 = 0.75;

$C_m = C_{mz1}+C_{mz2}*F_z+C_{mz3}*F_z^2$ with C_{mz1} = 2.9000; C_{mz2} = -3.4651e-4; C_{mz3} = 2.4648e-8;

$E_m = E_{mz1}+E_{mz2}*F_z+E_{mz3}*F_z^2$ with E_{mz1} = -1.6529; E_{mz2} = 4.4396e-6; E_{mz3} = -2.3414e-8;

b_1 = -0.0026058; b_2 = 56.1982; b_3 = 0;

b_4 = 166303; b_5 = 3826.8;

b_6 = -4.8699e-5; b_7 = 1.37723; b_8 = -1.24221e-4;

b_9 = 0.00005; b_{10} = 0.5;

b_{11} = -9.0889e-5; b_{12} = 1.96015;

b_{13} = -0.0001227; b_{14} = 1.96015;

b_{15} = 8.04018e-6; b_{16} = 7.7895e-3;

κ_p = 0.13; $\alpha_p = 0.000019463.F_z+0.054238$.

From these data, any steady state shear forces and aligning moments desired can be generated, via the algorithm, taken from reference [**2**], given in the Appendix. Examples are given in Figs 7 to 10.

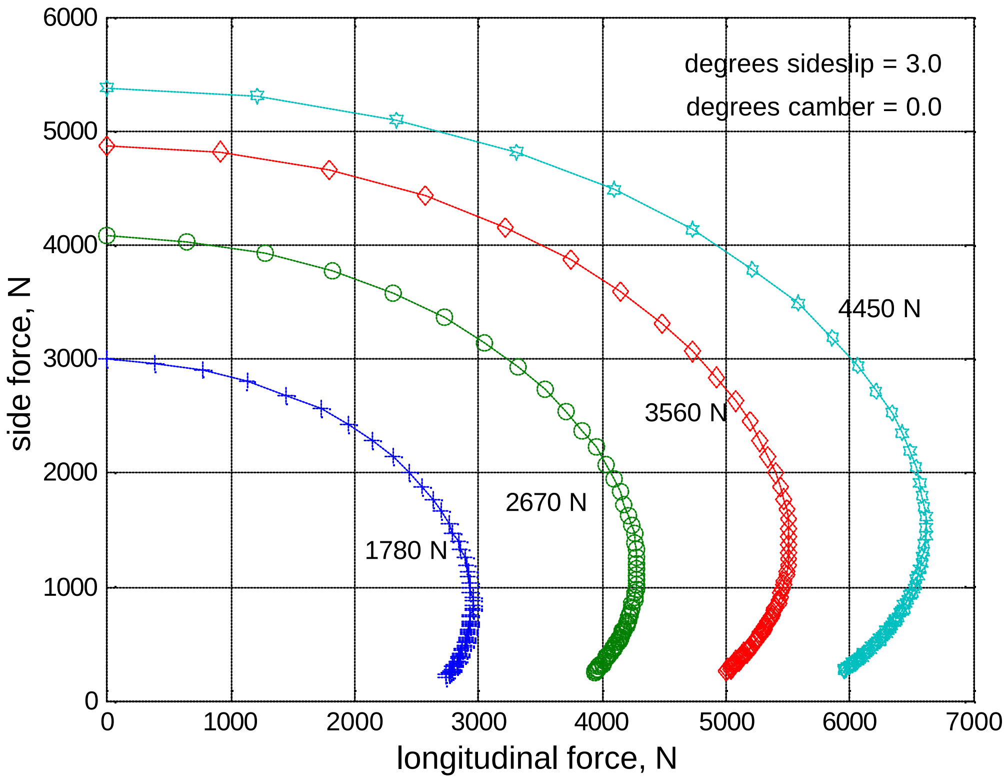

Fig. 7 Shear forces for 3 degrees sideslip and no camber, with longitudinal slip varying from 0 to 1 and four loads as shown

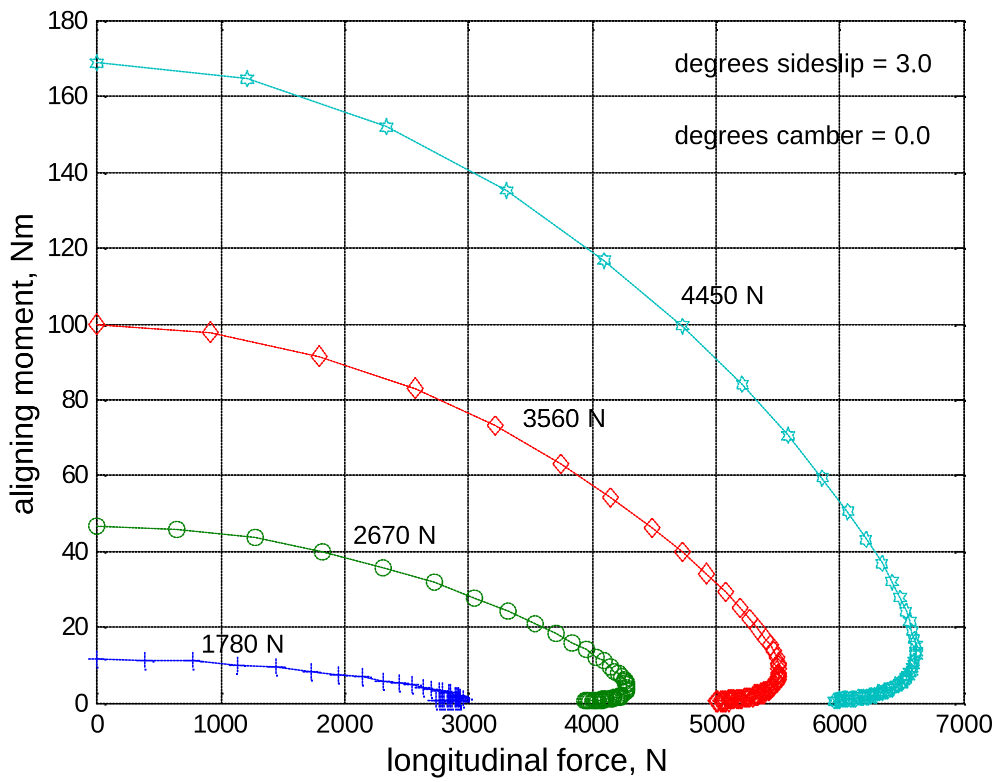

Fig. 8 Aligning moments for 3 degrees sideslip and no camber, with longitudinal slip varying from 0 to 1 and four loads as shown

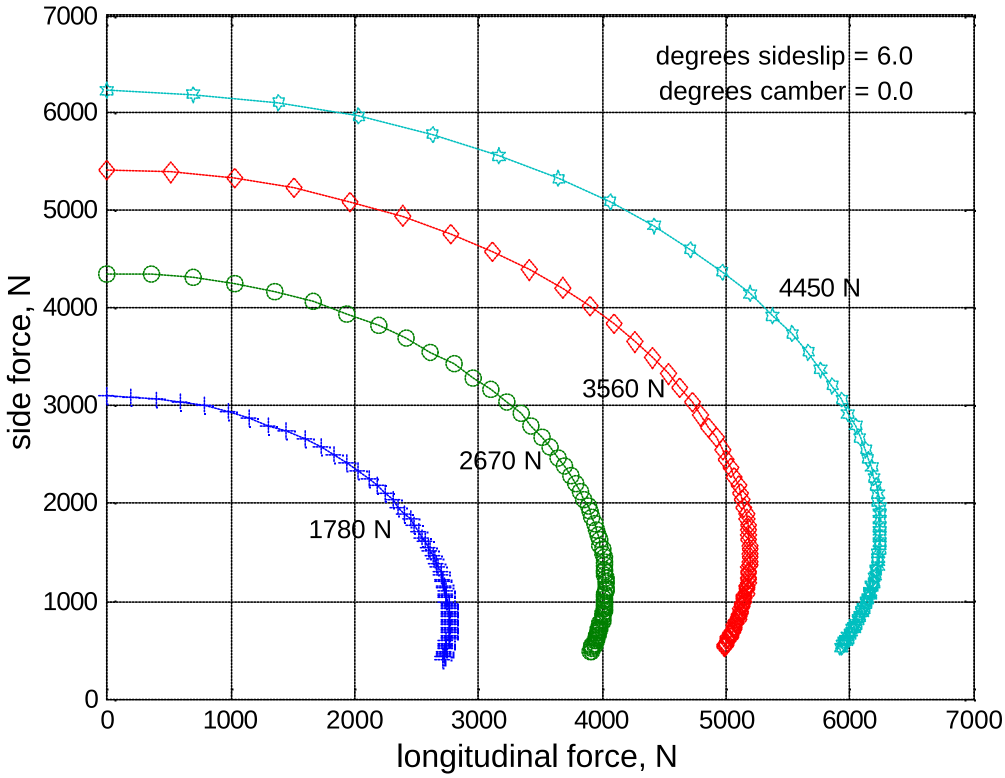

Fig. 9 Shear forces for 6 degrees sideslip and no camber, with longitudinal slip varying from zero to 1 and four loads as shown

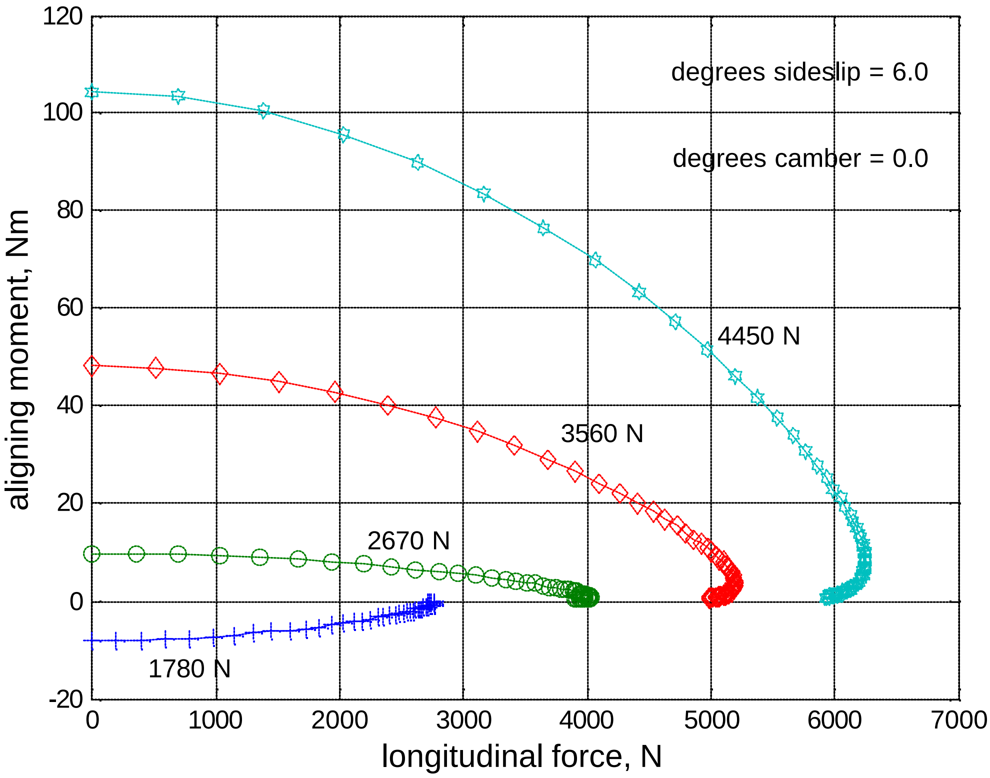

Fig. 10 Aligning moments for 6 degrees sideslip and no camber, with longitudinal slip varying from 0 to 1 and four loads as shown

4 RESULTS FOR A SECOND TYRE

To establish some degree of general applicability, a second tyre from the same source is examined in a similar fashion. The tyre in question is a Goodyear Eagle P275/40 ZR Corvette tyre (see reference [**1**], figure 2.44). In the first stage, C, E, b_4, b_5, b_{13} and b_{14} are identified from the experimental side force data. The best fit parameters, C = 2.324, E = 0.2128, b_4 = 164545, b_5 = 16594, b_{13} = -1.019e-5 and b_{14} = 1.0561, allow the reconstruction shown in Fig. 11. The fit is almost perfect but the relatively high value of C corresponds to a basic Magic Formula curve shape more representative of an aligning moment than a side force. In particular, for high positive slip values, negative forces would occur. High slip force values would be unreasonable with such a representation. Therefore, the value of C is constrained to 1.65 and a new optimization of the remaining parameters carried out. This gives almost as good a fit as the original, shown in Fig. 12. Clearly, with forces measured only up to the peak, C and E can be traded off against each other, without the fit quality altering much. C can be fixed, if desired, to control the high slip force behaviour of the tyre.

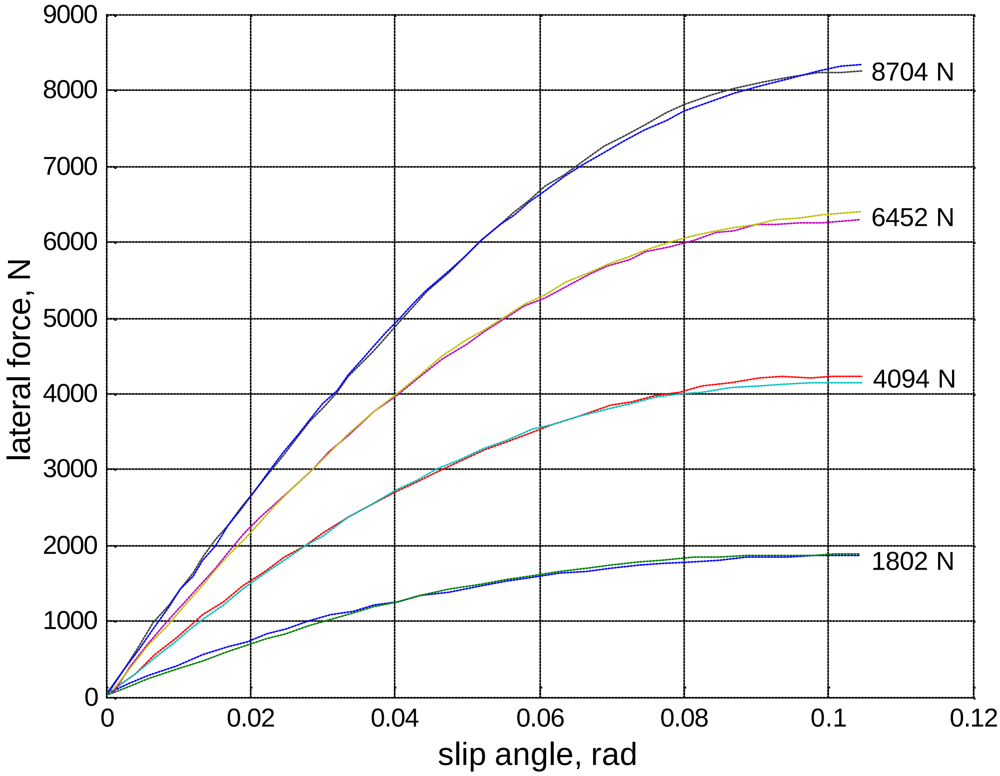

Fig. 11 Reconstructed side forces for best fit C, E, b_4, b_5, b_{13} and b_{14}. Solid lines show the experimental results from reference [**1**]; Dotted lines show the fitted results

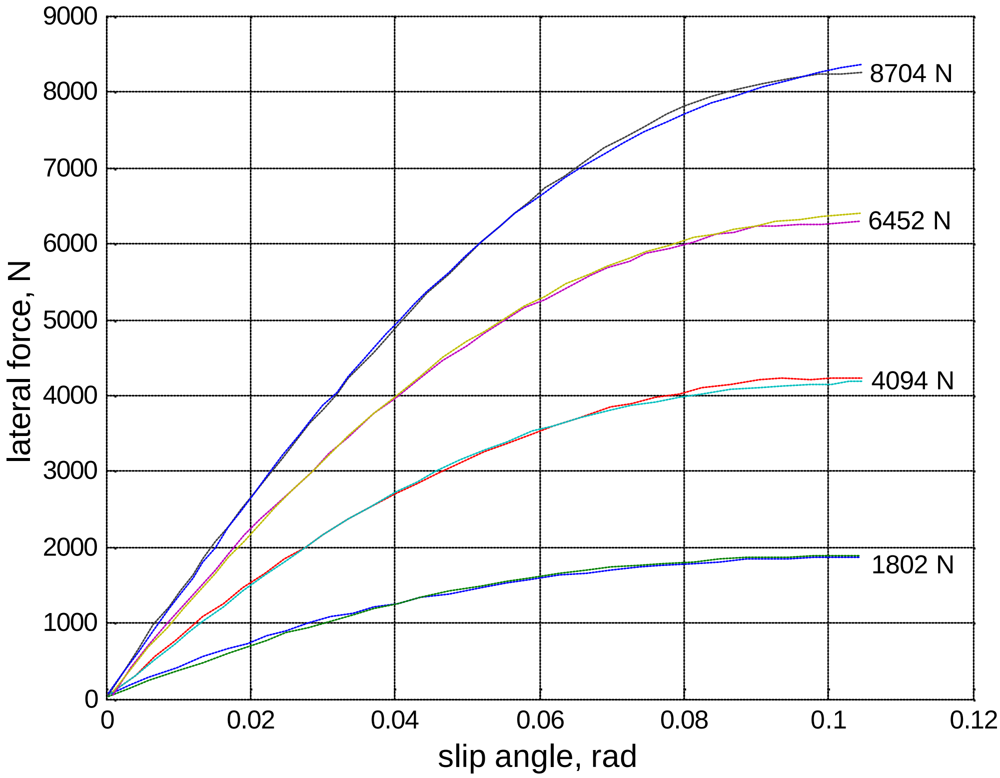

Fig. 12 Side forces for best fit E, b_4, b_5, b_{13} and b_{14} (see below for coefficients) with C constrained to be 1.65. Dotted lines show the fitted results

The aligning moment data allows the identification of the quadratic polynomial coefficients of expressions for C_m and E_m and the parameters b_6, b_7, b_8, b_{15} and b_{16}, with the results shown in Fig. 13. As with the Goodyear race tyre, the quadratic variation of C_m and E_m with load is necessary to get a good fit.

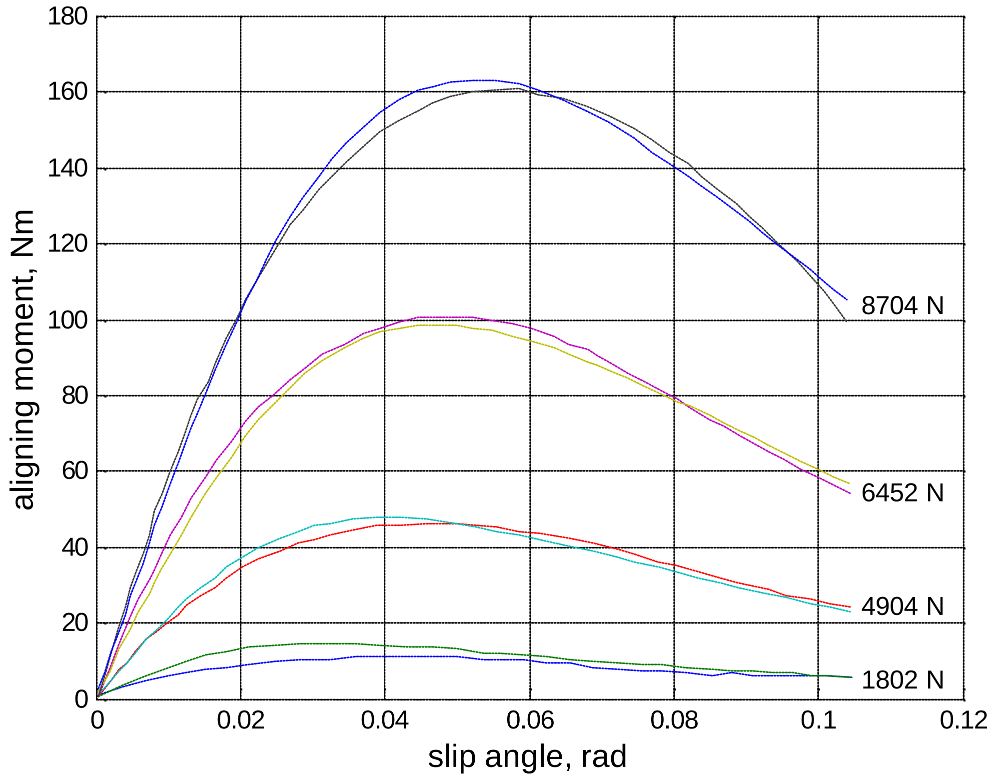

Fig. 13 Aligning moments for quadratic C and E values: Solid lines are for experimental results, while dotted lines are reconstructed

From the established values of b_{13} and b_{14}, D_y is obtained, while from b_4 and b_5, C_{fa} follows. Then, the Magic Formula relationship: $C_{fa} = B_y C D_y$ gives B_y. Equation (4) can next be solved for a_p for each of the four standard loads and polynomial fitting allows the description of a_p as a continuous function of load. The polynomial order is not restricted in any way. In this case, a quadratic gives an excellent fit to the four points.

As with the Goodyear race tyre treated above, it is considered most reasonable, in the absence of longitudinal force measurements, to take $b_{12} = b_{14}$. The value of b_{13} identified shows that the peak sideforce is almost proportional to the tyre load. It is invariably degressive, to some extent. In this case, that extent is very small. Taking the view that the rate of reduction in peak longitudinal force with increasing load will be less than that for the lateral force, little scope is left for varying b_{11}. It must be negative to get the normal degressive behaviour, while it must be numerically small to compare properly with the lateral properties. An estimate of b_{11} giving 4.2% more peak longitudinal force than peak lateral force at the highest load of 8702 N is made on this basis. Further, a reasonable estimate of the slip ratio for maximum longitudinal force, bearing in mind the rather strong dependence of a_p on load for this tyre, is that k_p will be proportional to load according to $k_p = 0.1176 + 1.4282e - 6.F_z$.

Putting the relevant values of C, E and k_p into equation (4) allows solving for B_x, giving C_{fk} *as* $B_x.C.D_x$ and the optimal coefficients b_1, b_2 and b_3 relating $C_{f\kappa}$ to load can then be found via “fminsearch”. Camber influences are dealt with as for the Goodyear race tyre, with a similar outcome, that $g_1 = 0.75$, $b_9 = 5e\text{-}5$ and $b_{10} = 0.5$. Slip_m follows from solution of (4), with C, E and B=1/C given for the normalized Magic Formula.

Now the data set is complete as follows:

C = 1.65; B = 1/C; E = -0.44939; slip_m = 2.0563; $g_1 = 0.75$;

$C_m = C_{mz1}+C_{mz2}*F_z+C_{mz3}*F_z^2$ with $C_{mz1} = 2.2299$; $C_{mz2} = 7.9288e\text{-}5$; $C_{mz3} = 8.8059e\text{-}10$;

$E_m = E_{mz1}+E_{mz2}*F_z+E_{mz3}*F_z^2$ with $E_{mz1} = 0.2852$; $E_{mz2} = 1.4025e\text{-}5$; $E_{mz3} = -1.9189e\text{-}10$;

$b_1 = 1.8532e\text{-}9$; $b_2 = 18.4831$; $b_3 = 1.5889e\text{-}5$;

$b_4 = 163179$; $b_5 = 16433$;

$b_6 = -2.1678e\text{-}8$; $b_7 = 0.4772$; $b_8 = -3.4432e\text{-}5$;

$b_9 = 0.00005$; $b_{10} = 0.5$;

$b_{11} = -4.7248e\text{-}6$; $b_{12} = 1.0588$;

$b_{13} = -9.4496e\text{-}6$; $b_{14} = 1.0588$;

$b_{15} = 1.5556e\text{-}6$; $b_{16} = 5.205e\text{-}3$;

$\kappa_p = 1.4282e\text{-}6.F_z+0.11757$; $\alpha_p = 3.4735e\text{-}10.F_z^2-7.03465e\text{-}7.F_z+0.10927$.

Combined slip forces and aligning moments derivable from this parameter set are illustrated in Figs 14 and 15 for an arbitrary sideslip angle of 5 degrees (0.0873 rad). Agreement of the results with the original measurements can be seen to be very good for both side forces and aligning moments, by comparison of these results with those of Figs 12 and 13 for pure sideslip. The continuity of the forces and moments as the slip ratio increases is also in evidence and the very high slip behaviour can be seen to be utterly reasonable in a qualitative sense.

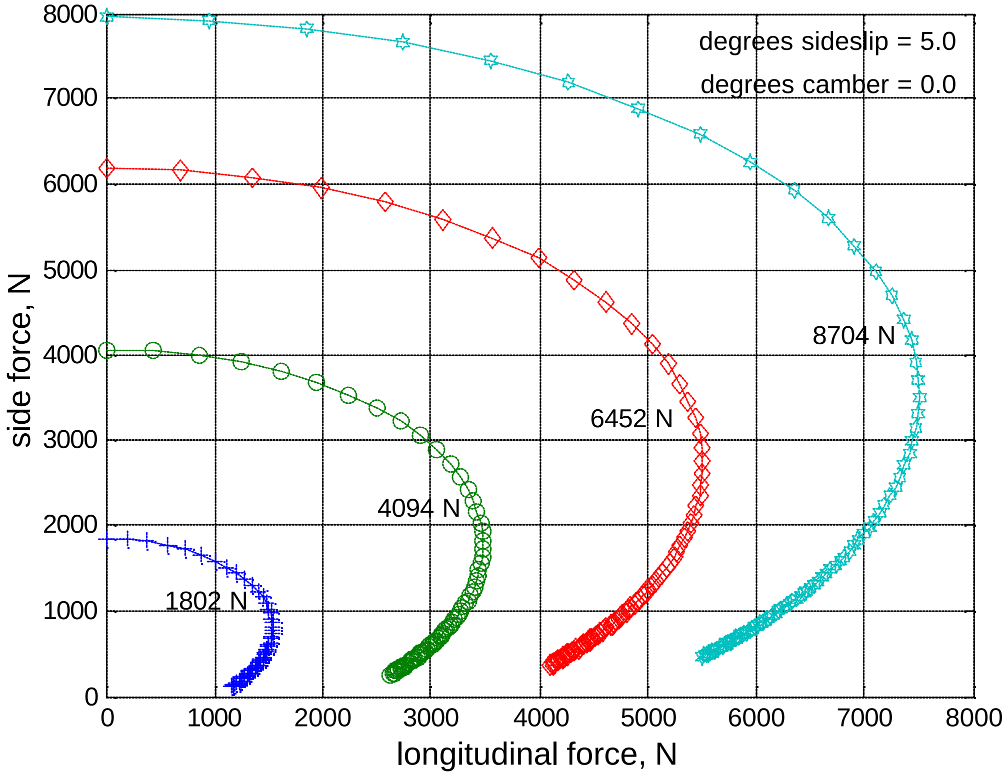

Fig. 14 Sideforce and braking force for 5 degrees sideslip angle and slip ratios from 0 to 1, reconstructed from the optimal parameter set

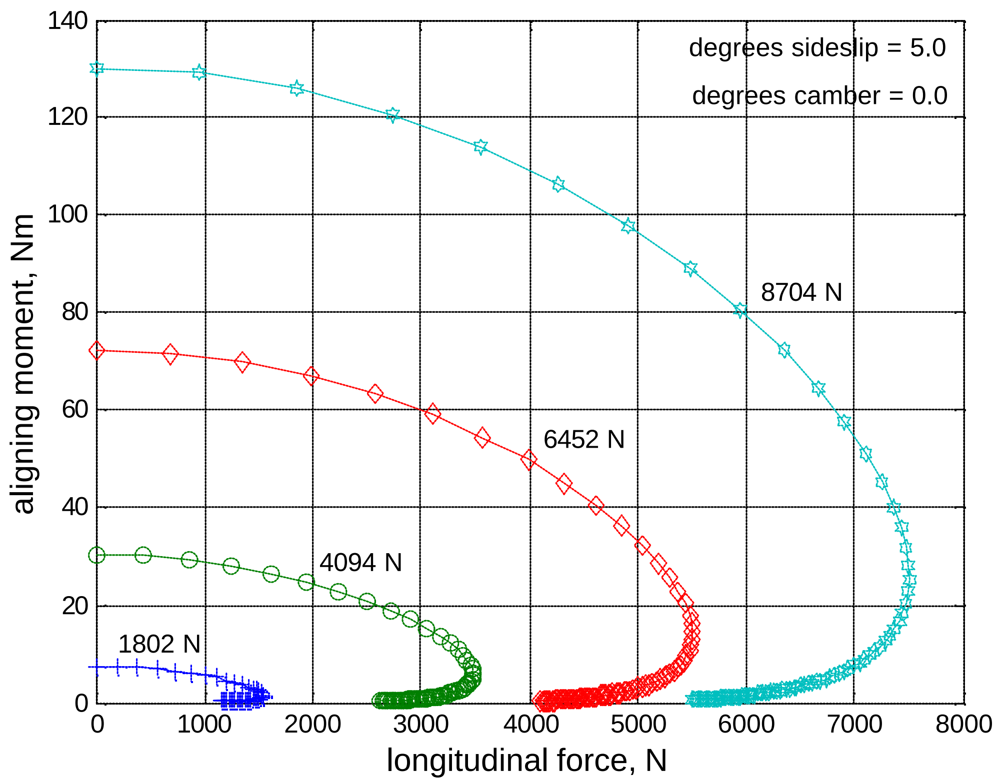

Fig. 15 Aligning moment for 5 degrees sideslip angle and slip ratios from 0 to 1, reconstructed from the optimal parameter set

5 CONCLUSIONS

Methods for the reconstruction of reasonably accurate, comprehensive, steady state, tyre shear force and moment characteristics from very modest data sources have been established and demonstrated. The methods are based on the combination of the Magic Formula and normalization of parameters described in reference [**2**], with non-linear slip transformations being central to the operation.

Two tyres, the basic side force and aligning moment properties of which are given in reference [**1**], have been used as examples, illustrating how the basic data, the Magic Formula expressions and fundamental knowledge of tyre mechanics can be brought to bear on the problem of deriving a good set of parameters. Standard optimization software is needed to make the method practical. The parameter set is easily convertible to tyre forces and moments through the algorithm given, which is a small development of that in reference [**2**].

The shear forces and moments for pure lateral slip are recoverable without significant distortion, through the normalization and de-normalization processes. The shear forces associated with longitudinal slip have had to be estimates and results based on these estimates have been shown to be quantitatively reasonable and qualitatively excellent. The analyst has some choice in accentuating the accuracy of one or other aspect of the tyre force system. In the circumstances in which the data used is entirely lateral force and aligning moment results and parameters are chosen to match those results closely, no loss of precision is implied by using the combined slip model, if the longitudinal slip values are small.

Comprehensive and useful tyre steady state shear force data can now be derived from very limited measurements.

References

1 Milliken, W. F. and Milliken, D. L. *Race Car Vehicle Dynamics*, 1996 (SAE, Warrendale).

2 Sharp, R. S. and Bettella, M. Tyre shear force and moment descriptions by normalization of parameters and the “Magic Formula”, *Vehicle System Dynamics,* in press.

3 Pacejka, H. B. and Bakker, E. The Magic Formula tyre model, Proc. 1st International Tyre Colloquium (H. B. Pacejka ed.), Delft, 1991, 1-18 (Supplement to *Veh. Syst. Dynamics*, **21**, Swets and Zeitlinger, Lisse).

4 Radt, H. S. and Glemming, D. A. Normalisation of tire force and moment data, *Tire Sci. and Technol.*, TSTCA, 1993, **21**(2), 91-119.

5 Pacejka, H. B. and Sharp, R. S. Shear force generation by pneumatic tyres in steady state conditions: a review of modeling aspects, *Veh. Syst. Dynamics*, 1991, **20**, 121-176.

6 Genta, G. *Motor Vehicle Dynamics: modeling and simulation*, 1997 (World Scientific Publishing, Singapore).

7 Clark, S. K. *Mechanics of Pneumatic Tires* 2nd edition, 1981, NBIS Monograph 122 (Washington DC).

8 Bakker, E., Nyborg, L. and Pacejka, H. B. Tyre modelling for use in vehicle dynamics studies, SAE 870421, 1987.

Appendix – MATLAB function for calculation of forces and moment

```
function [Fx,Fy,Mz] = norm_alg(fz,kappa,alpha,gamma);

% Tyre shear force / moment calculations via Magic Formula and similarity method

C_fkappa = fz*(b1*fz+b2)/exp(b3*fz);
C_falpha = b4*sin(2*atan(fz/b5));
C_malpha = fz*(b6*fz+b7)/exp(b8*fz);
C_fgamma = fz*(b9*fz+b10);
C_m = C_mz1+(C_mz2+C_mz3*fz)*fz;
D_fx = fz*(b11*fz+b12);
D_fy = fz*(b13*fz+b14);
D_mz = fz*(b15*fz+b16);
E_m = E_mz1+(E_mz2+E_mz3*fz)*fz;

a_feq = alpha+gamma*(C_fgamma+g1*fz)/C_falpha;

if alpha == 0
   alpha = eps;
```

```
end

Da_eq = D_fy+fz*g1*abs(gamma)*sign(alpha*gamma);

c_k = log(slip_m*D_fx/(k_p*C_fkappa))/k_p;
c_a = log(slip_m*Da_eq/(a_p*C_falpha))/a_p;
m_k = C_fkappa*exp(c_k*k_p)*(1+c_k*k_p)/D_fx;
m_a = C_falpha*exp(c_a*a_p)*(1+c_a*a_p)/Da_eq;
int_k = (C_fkappa*exp(c_k*k_p)/D_fx-m_k)*k_p;
int_a = (C_falpha*exp(c_a*a_p)/Da_eq-m_a)*a_p;

if a_feq < a_p
   a_feq_bar = C_falpha*a_feq*exp(c_a*a_feq)/Da_eq;
else
   a_feq_bar = m_a*a_feq+int_a;
end

B_fy = C_falpha/(C*D_fy);
phi_f = (1-E)*a_feq+(E/B_fy)*atan(B_fy*a_feq);
Fy0 = Da_eq*sin(C*atan(B_fy*phi_f));
B_mz = C_malpha/(C_m*D_mz);
phi_m = (1-E_m)*alpha+(E_m/B_mz)*atan(B_mz*alpha);
Mz0 = -D_mz*sin(C_m*atan(B_mz*phi_m));

if kappa < k_p
   k_bar = C_fkappa*kappa*exp(c_k*kappa)/D_fx;
else
   k_bar = m_k*kappa+int_k;
end
```

```
l_bar = sqrt(a_feq_bar^2+k_bar^2);
phi_bar = (1-E)*l_bar+(E/B)*atan(B*l_bar);
Fs = sin(C*atan(B*phi_bar));
Fx = D_fx*Fs*k_bar/l_bar;
Fy = Da_eq*Fs*a_feq_bar/l_bar;

if Fy0 == 0
   Fy0 = eps;
end

Mz = Mz0*(Fy/(Fy0))^2;
%*** *** ***
```